Int. J. Heat Mass Transfer. Vol. 3, pp. 42–54. Pergamon Press 1961. Printed in Great Britain.

RADIATIVE HEAT EXCHANGE BETWEEN SURFACES WITH SPECULAR REFLECTION

E. R. G. ECKERT* and E. M. SPARROW*

Heat Transfer Laboratory, Department of Mechanical Engineering,
University of Minnesota, Minneapolis, Minnesota

(*Received* 14 *July* 1960; *and in revised form* 13 *January* 1961)

Abstract—A method has been developed for calculating the radiant interchange in an enclosure containing specularly reflecting surfaces. Consideration is given to systems composed of two specular surfaces and an unrestricted number of black surfaces. The method is illustrated by numerical examples and comparisons are made with the heat transfer results for diffusely reflecting surfaces.

Résumé—Une méthode de calcul des échanges thermiques par rayonnement, dans une enceinte ayant des surfaces à réflexion spéculaire, a été développée. Les systèmes composés de deux surfaces spéculaires et d'un nombre illimité de surfaces noires ont été considérés. La méthode est illustrée par des exemples numériques et les résultats sont comparés aux résultats de transmission de chaleur obtenus pour des surfaces à réflexion diffuse.

Zusammenfassung—Es wurde eine Methode entwickelt, den Strahlungsaustausch in einem von spiegelnd reflektierenden Oberflächen begrenzten Hohlraum zu berechnen. Besondere Berücksichtigung fanden Systeme aus zwei spiegelnden Oberflächen und einer unbeschränkten Zahl schwarzer Flächen. Die Methode wird durch numerische Beispiele erläutert und die übertragenen Wärmemengen werden mit denen diffus strahlender Oberflächen verglichen.

Аннотация—Разработан метод вычисления лучистого теплообмена между зеркально отражающими поверхностями. Рассмотрены системы, состоящие из двух зеркальных поверхностей и неограниченного количества чёрных поверхностей. Метод иллюстрируется численными примерами, даны сравнения с результатами по теплообмену для случая диффузно отражающих поверхностей.

NOMENCLATURE

- A surface area;
- e_b black-body emissive power;
- F angle factor;
- H incident radiant flux per unit time and area;
- h spacing between parallel plates;
- k summation index;
- L plate length
- Q overall rate of heat loss;
- q local heat loss rate per unit area;
- s distance between surface elements;
- T absolute temperature;
- X dimensionless distance, x/L;
- x co-ordinate measuring distance along plate;
- α absorptivity;
- γ spacing ratio, h/L;
- θ opening angle, see Fig. 7;
- ϵ emissivity;
- ϵ_i interchange emissivity;
- ρ reflectivity;
- σ Stefan–Boltzmann constant.

* Professor of Mechanical Engineering.

INTRODUCTION

ENERGY exchange by thermal radiation has in the literature been discussed almost exclusively for diffusely reflecting surfaces. Experiments [1, 2] on the spacial distribution of the reflected energy, on the other hand, indicate that the reflection on many surfaces of engineering importance actually is closer to the limit of specular than of perfectly diffuse reflection, even if this is not clearly evident by visual inspection of the surfaces. This will be amplified in the final section of the report.

The present paper develops a method of calculating the heat exchange between plane surfaces with specular reflection and presents numerical comparisons between specular and diffuse heat transfer results for a few typical geometries.

Before going into the analysis of the new calculation method, some consideration will be given to a geometry for which the analysis of radiative heat exchange with specular as well as diffuse reflection has been made in the past, namely, for two concentric cylinders or spheres. The relationships describing heat exchange by radiation between the two surfaces will be used to obtain information on the order of magnitude of the difference between specularly and diffusely reflecting surfaces.

Heat exchange between concentric spheres or cylinders with specularly and diffusely reflecting surfaces

We will consider two co-axial cylinders of infinite length or alternatively, two concentric spheres. The relations for these two geometries are identical and for the sake of simplicity we will in the future talk only about the spherical arrangement. Parameters for the inner sphere may be identified by a subscript 1 and those for the outer sphere by a subscript 2. A denotes the surface area, ϵ the surface emissivity, and e_b the black body emissive power (heat flux emitted per unit area and unit time). The heat loss of the inner surface 1 and the heat gain of the outer surface 2 is then described by the equation

$$Q = A_1 \, \epsilon_i \, (e_{b1} - e_{b2}). \tag{1}$$

The equations which specify the interchange emissivity ϵ_i are derived in the various textbooks on heat transfer for the situation where the surfaces emit according to Lambert's cosine law (for instance in Ref. 3). The relation for diffusely reflecting surfaces is

$$\frac{1}{\epsilon_i} = \frac{1}{\epsilon_1} + \frac{A_1}{A_2}\left(\frac{1}{\epsilon_2} - 1\right) \tag{2}$$

and for specularly reflecting surfaces

$$\frac{1}{\epsilon_i} = \frac{1}{\epsilon_1} + \frac{1}{\epsilon_2} - 1. \tag{3}$$

Introduction of monochromatic emissivities and emissive powers into those equations results in the heat exchange in a small band at a certain wave length. Usually, engineering calculations require knowledge of the total amount of energy transfer in the whole wave length range. For gray surfaces with emissivities independent of wave length, equation (1) specifies this energy exchange provided that total emissive powers are introduced into this equation. They are described by Stefan–Boltzmann's relation $e_b = \sigma T^4$. For surfaces with wave length-dependent emissivities, the radiative heat loss Q has to be calculated with equations (1) to (3) at first for monochromatic radiation, and the total heat loss is obtained by an integration of the monochromatic heat loss over the whole wave length range. This statement holds not only for the present section, but for all calculations in this paper.

The relations (1) to (3) may be used to establish the extent of the differences between specularly and diffusely reflecting surfaces which can be expected for the specific geometry. For the limiting situation that the inner sphere is very small compared to the outer one ($A_1/A_2 \to 0$), the relation for the interchange emissivity in diffuse reflection is $\epsilon_i = \epsilon_1$. Equation (3) remains unchanged. If one specifies in addition that both surfaces have the same emissivity ($\epsilon_2 = \epsilon_1$), equation (3) becomes $(1/\epsilon_i) = (2/\epsilon_1) - 1$. For small values of ϵ_1 the relation is approximated by $\epsilon_i = \epsilon_1/2$. This indicates that heat exchange for diffusely reflecting surfaces with equal emissivities is in the present geometry up to two times as large as for specularly reflecting surfaces.

The differences may become even larger when the emissivities of the two surfaces have different values. Let us assume surface 1 to be a black surface ($\epsilon_1 = 1$). This makes the interchange emissivity for diffuse reflection and $A_1/A_2 \to 0$ also equal to 1. The interchange emissivity ϵ_i for specularly reflecting surfaces, on the other hand, is equal to ϵ_2. It may, therefore, be by an order of magnitude smaller for specular reflection, when the emissivity ϵ_2 has a small value.

The differences which have just been established are, of course, extremes. It can, however, easily be checked that differences of the same order of magnitude may arise even

when the ratio of the two surface areas is not extremely small and when the emissivities have other values. It can also be expected that the geometries investigated in this section exhibit differences which will not be reached for other geometries. A slight eccentricity of the two surfaces, for instance, should bring the heat fluxes for diffuse and specular reflection more closely together.

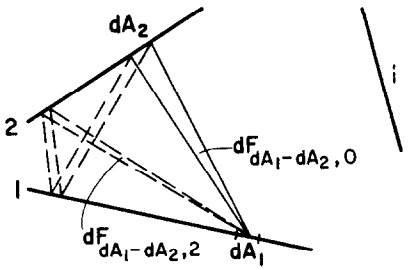

Fig. 1. Typical enclosure with two non-black surfaces.

HEAT EXCHANGE BETWEEN PLANE SURFACES WITH SPECULAR REFLECTION

Radiant interchange process

Consider a space which is enclosed by a number of plane surfaces. The temperature may be locally uniform on each of the surfaces, but may be different for the various surfaces. The space is filled by a medium which is perfectly transmittant and which does not participate in the radiative energy exchange. The surfaces emit energy by thermal radiation and the directional distribution of the emitted energy flux may follow Lambert's cosine law.* The analysis in this paper will be developed for an enclosure with two specular-reflecting surfaces, assuming that the rest of the surfaces are black. A calculation for a larger number of reflecting surfaces is straightforward, but soon becomes exceedingly involved. We will start by a consideration of the energy exchange between the two reflecting surfaces. Fig. 1 is a sketch of the two surfaces 1 and 2. Two area elements dA_1 and dA_2 may be located on the two surfaces. The heat flux emitted by the surface element dA_2 and traveling toward the element dA_1 can be expressed as

$$\epsilon_2 \, e_{b2} \, dA_2 \, dF_{dA_2-dA_1,0} \tag{4a}$$

where $dF_{dA_2-dA_1,0}$ denotes an "angle factor", i.e. that fraction of the energy emitted by dA_2 which impinges on dA_1. The first subscript $dA_2 - dA_1$ indicates radiative exchange between areas dA_2 and dA_1; while the second subscript 0 denotes direct interchange with zero reflections.

Introducing the reciprocity relationship (Ref. 3, pp. 396–397)

$$dA_2 \, dF_{dA_2-dA_1} = dA_1 \, dF_{dA_1-dA_2}$$

expression (4a) can be rephrased as

$$\epsilon_2 \, e_{b2} \, dA_1 \, dF_{dA_1-dA_2,0}. \tag{4b}$$

The surface element dA_1 receives, in addition, radiative energy from dA_2 in an indirect way, for instance, on the path indicated by the dashed lines in Fig. 1. The energy arriving after two reflections is

$$\epsilon_2 \, e_{b2} \, \rho_1 \rho_2 \, dF_{dA_1-dA_2,2} \, dA_1 \tag{5}$$

$dF_{dA_1-dA_2,2}$ indicates the angle factor for the radiation traveling the dashed path in Fig. 1, with the second subscript 2 signifying that there have been two reflections. Energy also arrives at dA_1 after a larger number of reflections, for instance, after $2k$ reflections:

$$\epsilon_2 \, e_{b2} \, \rho_1^k \rho_2^k \, dF_{dA_1 \; dA_2,2k} \, dA_1. \tag{6}$$

The total energy emitted by dA_2 and arriving at dA_1 per unit area is obtained by a summation

$$\epsilon_2 \, e_{b2} \sum_0^\infty \rho_1^k \, \rho_2^k \, dF_{dA_1-dA_2,2k}. \tag{7}$$

The energy emitted by the whole surface area 2 and arriving at a unit area of dA_1 is

$$\epsilon_2 \, e_{b2} \sum_0^\infty \rho_1^k \, \rho_2^k \, F_{dA_1-A_2,2k} \tag{8}$$

where $F_{dA_1-A_2,2k}$ expresses the angle factor for radiation leaving surface 2 and arriving at dA_1 after $2k$ reflections on surfaces 1 or 2.

The surface element dA_1 receives also radiant

* Surfaces may approach Lambert's Law in emission while approaching specularity in reflection; see for example, copper oxide in Figs. 13-12 and 13-13 of Ref. 3.

energy which originates at surface 1 and is reflected back to dA_1 by surface 2. The energy arriving is

after one reflection

$$\epsilon_1 e_{b1} F_{dA_1-A_1,1} \rho_2 \tag{9}$$

after three reflections

$$\epsilon_1 e_{b1} F_{dA_1-A_1,3} \rho_1 \rho_2^2 \tag{10}$$

after $2k + 1$ reflections

$$\epsilon_1 e_{b1} F_{dA_1-A_1,2k+1} \rho_1^k \rho_2^{k+1}. \tag{11}$$

The total amount of energy originating at surface 1 and arriving at dA_1 is again obtained by a summation

$$\epsilon_1 e_{b1} \sum_0^\infty \rho_1^k \rho_2^{k+1} F_{dA_1-A_1,2k+1}. \tag{12}$$

The surface element dA_1 will also receive radiation which is emitted by any of the black surfaces of the enclosure and arrives at the surface element after one or several reflections at surfaces 1 or 2. Let us consider the radiation originating from one of the black surfaces denoted by i. That part of the radiation for which the first reflection occurs at surface 2 can be treated formally in the same way as the expression (12), when the proper angle factor is introduced. The energy flux arriving at dA_1 after one or several reflections is

$$e_{bi} \sum_0^\infty \rho_1^k \rho_2^{k+1} F_{dA_1-A_i,2k+1}. \tag{13}$$

That part of the radiation for which the first reflection occurs at surface 1 will be described again by the same form as expression (8).

$$e_{bi} \sum_0^\infty \rho_1^k \rho_2^k F_{dA_1-A_i,2k}. \tag{14}$$

This expression also contains the radiation which arrives directly at dA_1.

The total flux H arriving at a unit area of surface 1 at the location of dA_1, either directly or after reflections from surfaces 1 and 2, can now be written as the sum of the expressions (8), (12), (13), and (14).

$$\left.\begin{aligned} H_1 = {} & \epsilon_1 e_{b1} \sum_0^\infty \rho_1^k \rho_2^{k+1} F_{dA_1-A_1,2k+1} \\ & + \epsilon_2 e_{b2} \sum_0^\infty \rho_1^k \rho_2^k F_{dA_1-A_2,2k} \\ & + \sum_{i=1}^n e_{bi} \Big[\sum_0^\infty \rho_1^k \rho_2^{k+1} F_{dA_1-A_i,2k+1} \\ & + \sum_0^\infty \rho_1^k \rho_2^k F_{dA_1-A_i,2k}\Big] \end{aligned}\right\} \tag{15}$$

The summation of radiation originating at black surfaces has to be extended over all n black surfaces. The net local heat loss per unit area at the element dA_1 finally can be expressed as the difference of the amount of radiation emitted by the surface and the amount absorbed by it.

$$q_1 = \epsilon_1 e_{b1} - \alpha_1 H_1. \tag{16}$$

The heat loss at any location of the reflecting surfaces can be calculated with equations (15) and (16) as soon as the various angle factors involved are known.

The overall net heat loss Q from surface 1 can be found from an equation similar to (16), with the modifications that the right side is multiplied by A_1 and the angle factors $F_{A_1-A_1}$, $F_{A_1-A_2}$, etc., are used in evaluating H. This same result can be obtained by integrating the local heat loss q over the area A_1.

Determination of angle factors

The angle factor for direct interchange $dF_{dA_1-dA_2,0}$ is given by the equation

$$dF_{d_1A-dA_2,0} = \frac{\cos\beta_1 \cos\beta_2}{\pi s^2} dA_2 \tag{17}$$

in which β denotes the angle between the line connecting the two area elements and the respective surface normal. s is the distance between the two surface elements. The angle factor $F_{dA_1-A_2,0}$ is obtained by an integration over the surface 2.

$$F_{dA_1-A_2,0} = \int_2 \frac{\cos\beta_1 \cos\beta_2}{\pi s^2} dA_2. \tag{18}$$

The angles β and the distance s have, of course, to be considered as functions of the location of dA_2.

The angle factor $F_{dA_1-A_2,\,2}$ is obtained by the following method, which is based on standard procedures in optics (see Fig. 2a). Consider the emitting area 2 as object and the planes 1 and 2 as mirrors. Mirror 1 creates an image 2_1 (Fig. 2a)

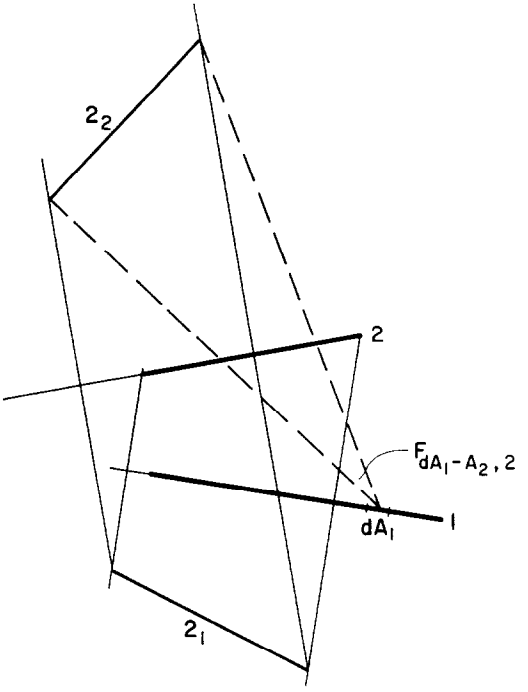

FIG. 2(a). Diagram illustrating angle factors $F_{dA_1-A_2,\,0}$ $F_{dA_1-A_2,\,2}$ etc.

of area 2. In turn, this first image 2_1 is reflected in mirror 2, creating image 2_2. The angle factor $F_{dA_1-A_2,\,2}$ is then identical with the angle factor between the area 2_2 and the element dA_1 for direct radiative interchange. It can be obtained from equation (18) when the area element dA_2 is located on the second image 2_2 and when the angle β_2 and the distance s are interpreted accordingly. Two more reflections on the mirrors 1 and 2 create a fourth image and the angle factor $F_{dA_1-A_2,\,4}$ is again identical with the angle factor for direct radiative interchange between the image 2_4 and the area element dA_1.

The angle factors $F_{dA_1-A_1,\,1}$, $F_{dA_1-A_1,\,3}$, and so on, are in the same way obtained by determination of the images 1_1, 1_3 and so on. Fig. 2(b) indicates the construction of these images.

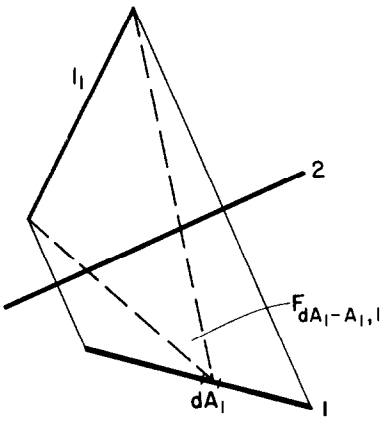

FIG. 2(b). Diagram illustrating angle factors $F_{dA_1-A_1,\,1}$ etc.

The angle factors $F_{dA_1-A,\,k}$ of any black surface are finally determined in the same way by constructing the images of the surface i in the mirrors 1 and 2.

In certain cases, the construction procedure as discussed above has to be modified to account for the fact that the participating areas may be too small to reflect the full images. Fig. 3

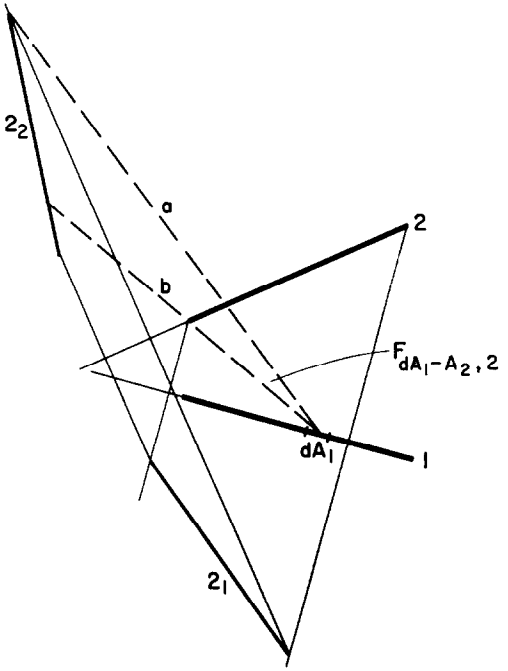

FIG. 3. Diagram illustrating partial use of images.

illustrates this point. Only that part of the image 2_2 between the rays a and b has to be used to determine the angle factor. Generally, that part of an image has to be considered from which the rays drawn towards the centre of dA_1 intersect area 2.

ILLUSTRATIVE RESULTS

It is useful to numerically illustrate the general method and, additionally, to make comparisons with results for diffusely reflecting surfaces. The particular situations treated below were selected on the basis of available exact solutions for gray, diffuse surfaces.

Two parallel plates of equal temperature

The sketch in Fig. 4 indicates two plates of width L arranged at a distance h. In the direction

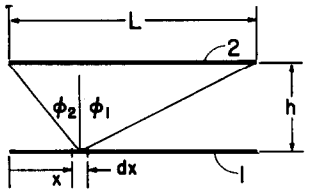

FIG. 4. Parallel plate system.

normal to the plane of drawing, the plates are taken to be infinite in extent. It will be assumed that the two plates are made of the same material so that they have equal radiation properties and that they are kept at the same temperature ($\epsilon_1 = \epsilon_2 = \epsilon$, $\rho_1 = \rho_2 = \rho$, $\alpha_1 = \alpha_2 = \alpha$, $e_{b1} = e_{b2} = e_b = \sigma T^4$). The surroundings of the plates may be at a temperature of absolute zero so that no radiation enters the space between the two plates from the outside. The same condition for radiative exchange holds when the two plates are connected at their rim by two black surfaces at absolute zero temperature. Later on, the results will be generalized to account for a black surrounding at arbitrary temperature. The angle factor for an area element dA located at a distance x from the rim of plate 1 is, according to Ref. 3, p. 401,

$$F_0 = \tfrac{1}{2}(\sin\varphi_1 + \sin\varphi_2). \tag{19}$$

The angles φ_1 and φ_2 can be expressed by the length dimensions to obtain

$$F_0 = \tfrac{1}{2}\left[\frac{x}{\sqrt{(x^2+h^2)}} + \frac{L-x}{\sqrt{\{(L-x)^2+h^2\}}}\right] \tag{20}$$

It is not necessary to differentiate between radiation originating at surface 1 or 2 since both are at the same temperature. Accordingly, only one subscript is used for the angle factors to indicate the number of reflections. For k reflections, the image is located at a distance $(k+1)\,h$. The angle factor for this image is

$$F_k = \tfrac{1}{2}\left[\frac{x}{\sqrt{\{x^2+(k+1)^2h^2\}}} + \frac{L-x}{\sqrt{\{(L-x)^2+(k+1)^2h^2\}}}\right]. \tag{21}$$

The total flux H arriving at a unit surface area at the location of dA is obtained from equation (15) which simplifies to the following expression if use is made of the fact that the two emissivities and emissive powers are equal, that e_{bi} is equal to zero, and that no differentiation has to be made between the two types of angle factors in this equation.

$$H = \epsilon\, e_b \sum_0^\infty \rho^k F_k. \tag{22}$$

The relation (16) then determines the heat loss of the surface at location dA with the expression (22) for the incident flux H and the relation (21) for the angle factors. The following equation is obtained when, in addition, dimensionless parameters are introduced to characterize the length dimensions: $X = x/L$, $\gamma = h/L$

$$\frac{q}{\epsilon\sigma T^4} = 1 - \frac{\alpha}{2}\left\{\sum_0^\infty \rho^k \left[\frac{X}{\sqrt{\{X^2+(k+1)^2\gamma^2\}}} + \frac{1-X}{\sqrt{\{(1-X)^2+(k+1)^2\gamma^2\}}}\right]\right\}. \tag{23}$$

The total heat loss of each one of the two plates is obtained in the same way by introducing the following relation for the average angle factor between two parallel plates

$$\bar{F}_k = \sqrt{\{1+(k+1)^2\gamma^2\}} - (k+1)\gamma = F_{A_1-A_2,\,k} \tag{24}$$

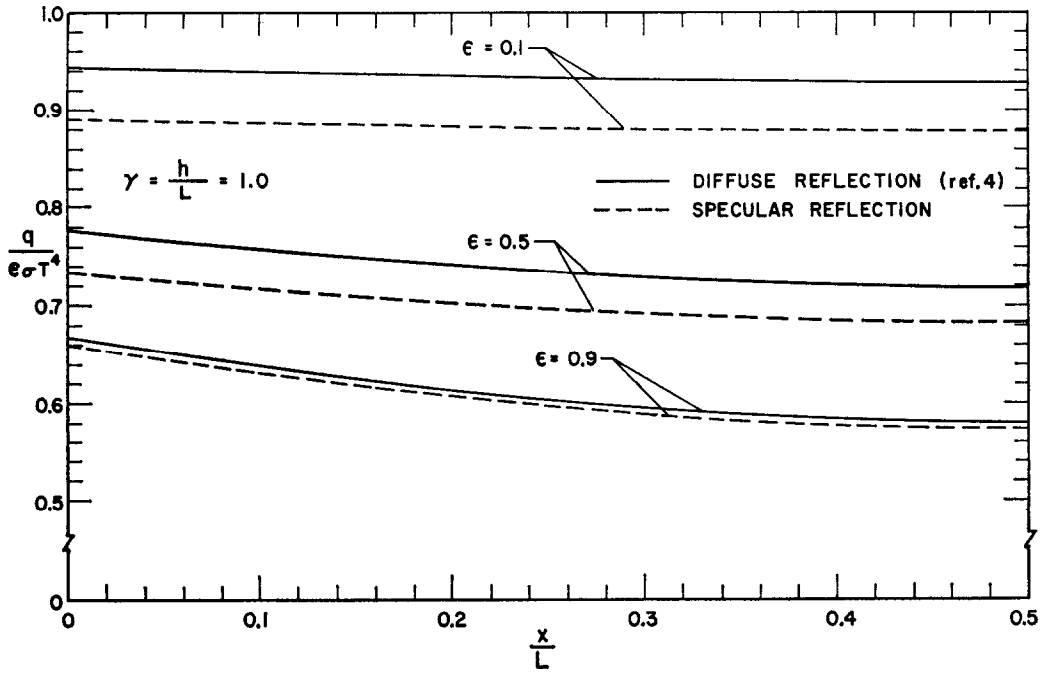

FIG. 5. Local heat flux results for parallel plate system with $\gamma = h/L = 1{\cdot}0$.

into equations (22) and (16). The following relation is obtained in this way

$$\frac{Q/L}{\epsilon\sigma T^4} = 1 - a \sum_0^\infty \rho^k \left[\sqrt{\{1+(k+1)^2\gamma^2\}} - (k+1)\gamma\right]. \quad (25)$$

The infinite series in equations (23) and (25) have been evaluated on an electronic computer, type Remington–Rand 1103. The local heat loss on any of the parallel plates, made dimensionless by the energy emitted from the surface, is plotted in Figs. 5 and 6 over the dimensionless distance from the plate rim. The first of these is for a wide spacing, $h/L = 1$, while the second is for a close spacing, $h/L = 0{\cdot}05$. Curves are presented for emissivities 0·1, 0·5, and 0·9 as dashed lines, and the heat losses encountered by diffusely reflecting plates are also shown for comparison purposes as full lines. This last information was taken from the analysis published in Ref. 4.

The curves in Fig. 5 indicate that the heat loss of parallel plates is larger when the plates reflect diffusely. This can be explained by the fact that at each diffuse reflection the impinging ray is distributed in all directions and that by this process, in the average, the radiative flux has a better chance to escape through the opening between the plates. Additionally, the level of the curves increases with decreasing ϵ (increasing reflectivity), since radiative energy escapes not only as direct radiation, but also in the subsequent reflections. This increase in the heat loss in either reflection process is very slight for $\epsilon = 0{\cdot}9$, as can be recognized by a comparison of the pertinent curves of Fig. 5 with the heat loss results for black surfaces ($\epsilon = 1$). A simple calculation determines the heat loss parameter of black plates as 0·646 for $X = 0$ and as 0·552 for $X = \frac{1}{2}$.

Figure 6 presents, in the same way, the results for a close spacing of the plates ($h/L = 0{\cdot}05$). It can be seen that near the rim of the plates the relative position of the curves for specular and for diffuse reflection is the same as for the wider spacing of Fig. 5. In the inner part, however, the trend reverses and the heat loss of the plates with specular reflection is larger than the heat loss of the diffusely reflecting plates. This may be

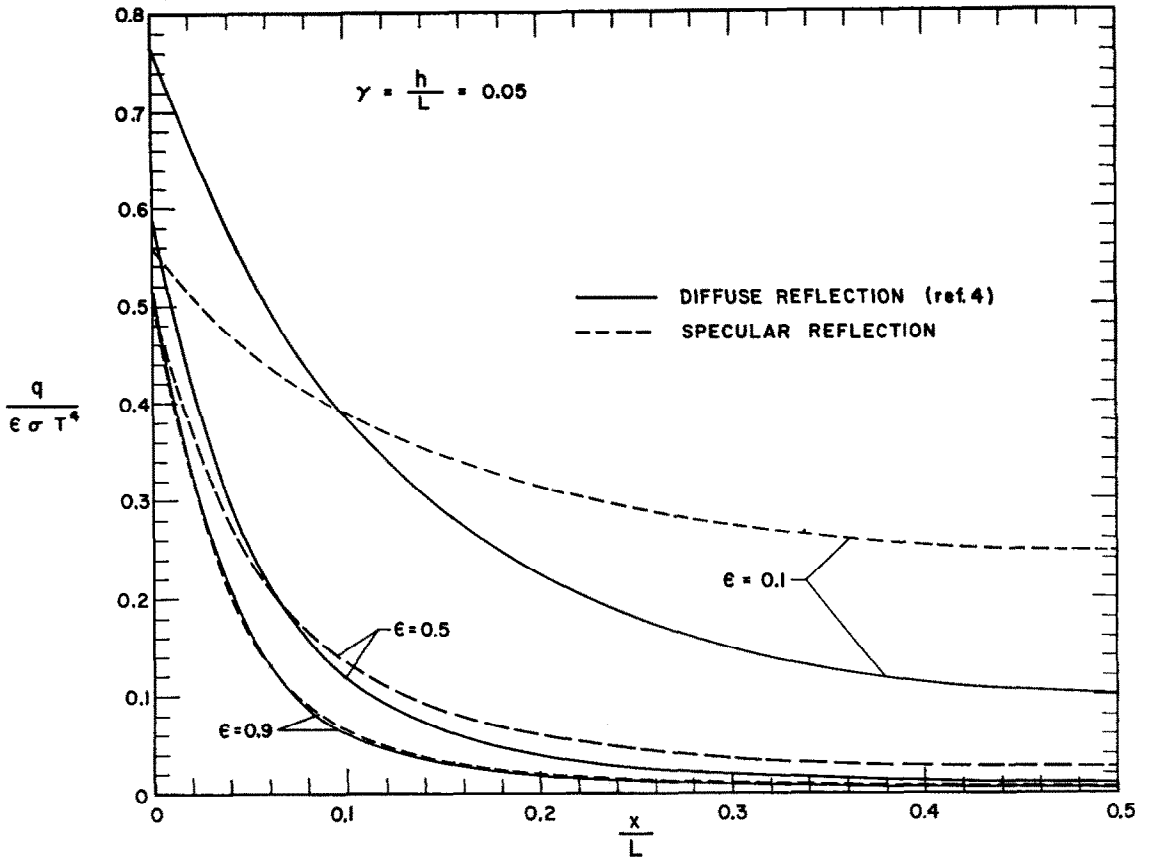

FIG. 6. Local heat flux results for parallel plate system with $\gamma = h/L = 0{\cdot}05$.

explained by the fact that radiation originating at the inner part of the plates escapes through the opening between the plates in general only after a larger number of reflections. The number of reflections, however, will, in an average, be smaller if the plates reflect specularly. It is again found that the curves for $\epsilon = 0{\cdot}9$ are located only slightly above the curve for $\epsilon = 1$, so that for this emissivity, reflections contribute only to a very small degree to the heat loss parameter.

The total heat loss from the surface of any plate has also been calculated from equation (25) and is presented in Table 1(a). The average heat flux Q/L per unit area and unit time has been divided by the energy flux leaving a unit area of a black surface at the plate temperature T. It is to be noted that the tabulated parameter has not been normalized by ϵ as were the ordinates of Figs. 5 and 6. Values for four plate spacings and for three emissivities have been entered for specular reflection as well as for diffuse reflection. Two sets of values for diffuse reflection were available from Ref. 4. One group of values presents the solutions of an integral equation describing the energy exchange process exactly. The second series of values results from a simplified analysis which neglects the local variation of the reflected radiative flux and replaces in this way the integral equation by an algebraic one. According to the specific definition of the heat loss parameter, the values of this parameter decrease with decreasing emissivity as contrasted to the behavior of the parameter presented in Figs. 5 and 6. The differences between specular and diffuse reflection are

Table 1. *Overall heat loss,* $(Q/L)/(\sigma T^4)$

(a) *Parallel plate system* (*Fig.* 4)

h/L	$\epsilon = 0{\cdot}1$			$\epsilon = 0{\cdot}5$			$\epsilon = 0{\cdot}9$		
	Specular	Diff. exact.	Diff. simpl.	Specular	Diff. exact.	Diff. simpl.	Specular	Diff. exact.	Diff. simpl.
1·0	0·08826	0·09338	0·09340	0·3503	0·3692	0·3694	0·5439	0·5500	0·5500
0·5	0·07948	0·08576	0·08607	0·2622	0·2747	0·2764	0·3632	0·3658	0·3664
0·1	0·04735	0·0442	0·05122	0·08575	0·07964	0·08677	0·09393	0·09269	0·09402
0·05	0·03220	0·0252	0·03388	0·04631	0·04128	0·04649	0·04848	0·04751	0·04848

(b) *Adjoint plate system* (*Fig.* 7)

θ	$\epsilon = 0{\cdot}1$			$\epsilon = 0{\cdot}5$			$\epsilon = 0{\cdot}9$		
	Specular	Diff. exact.	Diff. simpl.	Specular	Diff. exact.	Diff. simpl.	Specular	Diff. exact.	Diff. simpl.
135°	0·0992	0·0992	0·0992	0·481	0·480	0·480	0·838	0·838	0·838
90°	0·0971	0·0958	0·0960	0·427	0·412	0·414	0·663	0·655	0·656
60°	0·0938	0·0899	0·0909	0·358	0·327	0·333	0·484	0·472	0·474
45°	0·0906	0·0838	0·0861	0·304	0·268	0·277	0·376	0·365	0·367

largest for a close spacing and for a small emissivity. For $h/L = 0{\cdot}05$ and $\epsilon = 0{\cdot}1$, the heat loss of the specularly reflecting surface is larger by 28 per cent than the exactly calculated value for diffuse reflection. For this case, the error which is made by the use of the simplified analysis for diffuse reflection is even larger than the difference between specular and diffuse reflection.

The information in Figs. 5 and 6 and in Table 1 can immediately be used to determine the heat loss from parallel plates for the situation that they are in energy exchange by radiation with a black environment at a temperature T_e. The only change which has to be made in equations (23) and (25) as well as in the figures and table is that the term σT^4 in the denominator has to be replaced by $\sigma(T^4 - T_e^4)$. This is immediately evident from the fact that radiation entering from the environment consists of rays which experience exactly the same fate as rays starting from the plate surfaces and traveling to the environment. One can also consider the situation that the environment and the plates are at the same temperature. In this case the geometry corresponds to an isothermal, closed "hohlraum" and no net heat flux can exist in such an enclosure according to the second law of thermodynamics.

Two plates forming a groove

Figure 7 indicates two plates of width L arranged in such a way that they form a groove

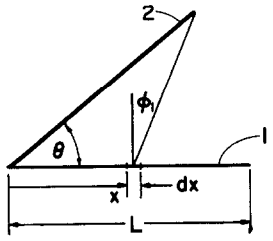

FIG. 7. Adjoint plate system.

with an opening angle θ. It will again be assumed that the plates have infinite length normal to the plane of drawing, and also, to provide comparisons with available diffuse results, that both

plates have equal and uniform temperatures. The angle factor under which an area element dA_1 sees the opposite plate is

$$F_{dA_1-A_2} = \tfrac{1}{2}(1 + \sin \varphi_1) \tag{26}$$

or expressed in the parameters $X = x/L$ and θ

$$F_{dA_1-A_2} = F_\theta = \tfrac{1}{2}\left\{1 + \frac{\cos\theta - X}{\sqrt{(1 - 2X\cos\theta + X^2)}}\right\}. \tag{27}$$

The situation in the present arrangement is different from the one in the previous section insofar that, after a finite number of reflections, an image is formed whose enveloping ray bundle as seen from dA_1 does not intersect the opposite surface. For an included angle of 90°, for instance, the image generated by the first reflection is already subject to this condition. Correspondingly, the heat flux q is described by the following equation which contains only the angle factor for direct radiative interchange

$$\frac{q}{\epsilon\sigma T^4} = 1 - \alpha F_{90°}. \tag{28}$$

For an included angle of 45°, the enveloping ray bundles drawn from dA_1 to the first and the second images 1_1 and 2_2 intersect the opposite plate. However, the enveloping ray bundles drawn from dA_1 to further images do not intersect A_2. Hence, the local heat loss q per unit area is described by an equation which contains three angle factors including the one for direct interchange as well as for the first image, which is a plate inclined under an angle $\theta = 90°$, and for the second image, which is a plate inclined under $\theta = 135°$

$$\frac{q}{\epsilon\sigma T^4} = 1 - \alpha(F_{45°} + \rho F_{90°} + \rho^2 F_{135°}). \tag{29}$$

The angle factors in equations (28) and (29) are obtained from equation (27) when the proper angle θ is inserted.

The results of the calculation are presented in Figs. 8 and 9, respectively, for 90° and 45° opening angles. The heat loss parameter has been calculated for emissivity values 0·1, 0·5, and 0·9. The dashed curves indicate the heat losses for specular reflection, and the corresponding

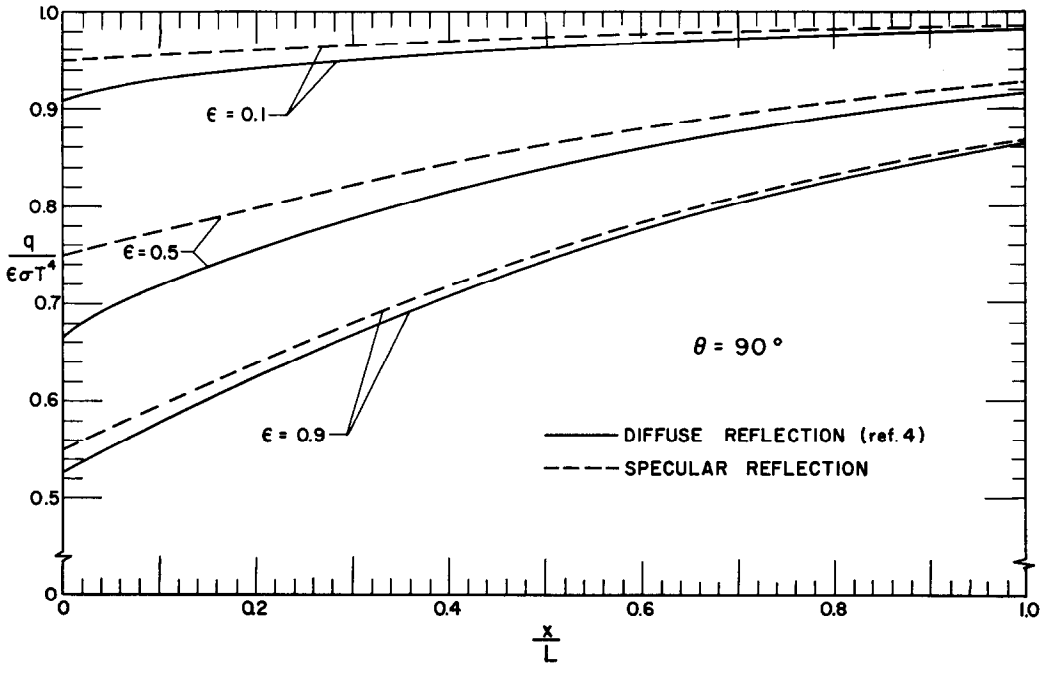

FIG. 8. Local heat flux results for adjoint plate system with $\theta = 90°$.

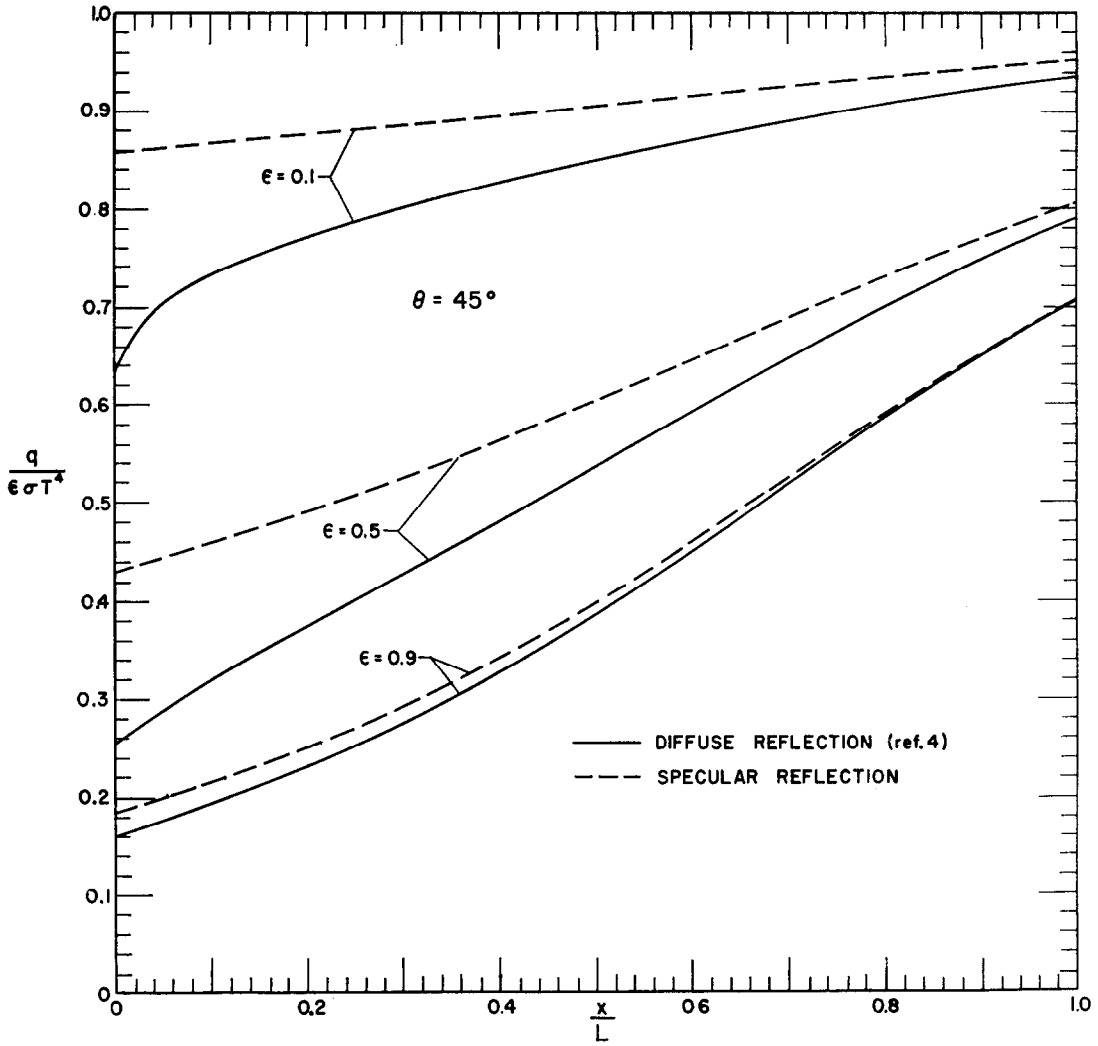

FIG. 9. Local heat flux results for adjoint plate system with $\theta = 45°$.

losses for diffuse reflection have again been entered as full lines for comparison purposes. These values have been taken from the analysis in Ref. 4. For both opening angles, the heat loss of plates with specular reflection is larger than the heat loss of diffusely reflecting surfaces. This is explained by the fact that the angular arrangement of the plates makes it easy for specularly reflected radiation to escape through the opening.

Table 1 (b) contains the average heat loss Q/L of the surfaces per unit area, divided by the energy emitted from a black surface at the specific temperature T. It should be noted that this parameter is not normalized by ϵ as were the ordinates of the figures. The results of calculations for four angles and for three emissivity values are presented. Results from Ref. 4 for diffuse reflection are also entered. The two columns for diffuse reflection present the results obtained by the solution of the integral equation and those from the simplified method. The heat loss parameter in this table compares the actual heat loss with the energy emitted by a

black surface, and it consequently decreases with decreasing emissivity values. The differences between specular and diffuse reflection are found to be largest for a small opening angle and for a low emissivity. The difference between the exact solution for diffuse reflection and the solution for specular reflection is 8 per cent for $\theta = 45°$ and $\epsilon = 0{\cdot}1$. Because the 45° angle is still a relatively open configuration, this difference is considerably smaller than the differences existing for concentric cylinders or spheres and also smaller than the differences between the closely spaced parallel plates.

ACTUAL DIRECTIONAL DISTRIBUTION OF REFLECTED RADIATION

Figures 10 and 11 present the angular distribution of reflected radiation for a few solid surfaces taken from Ref. 3. The curves have been

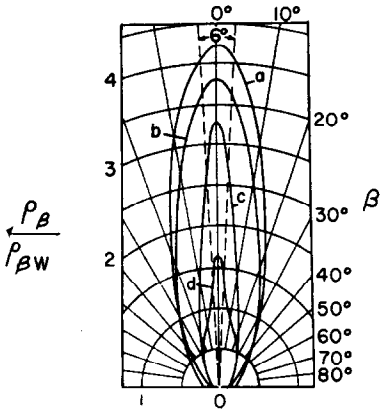

FIG. 10. Directional distribution of reflected radiation (black incident energy): *a*—aluminum paint; *b*—iron, scraped; *c*—black iron; *d*—copper oxide. ρ_β = measured reflectivity, $\rho_{\beta w}$ = reflectivity of a perfectly diffuse white surface. (From Ref. 3, Fig. 13-13).

obtained by directing a bundle of radiant energy with nearly normal incidence and with an opening angle of 6° towards the surface. The incident radiation came from a black body at the temperature 530°F and the reflecting surface was kept at atmospheric temperature. It can be recognized that the angular distribution of the reflected radiation for any of the surfaces is neither completely specular nor completely diffuse. The figures show that surfaces which appear specular to the eye approach more closely to specular reflection than to diffuse reflection for thermal radiation. But, even surfaces which appear diffuse to the eye (e.g. clay, scraped iron) may reflect a considerable

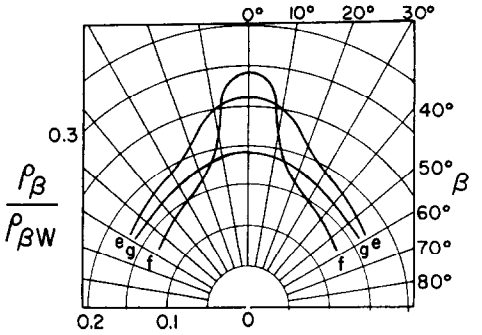

FIG. 11. Directional distribution of reflected radiation (black incident energy): *e*—cast iron; *f*—clay; *g*—wood. ρ_β = measured reflectivity. $\rho_{\beta w}$ = reflectivity of a perfectly diffuse white surface. (From Ref. 3, Fig. 13-14).

portion of thermal radiation in the proximity of the specularly reflected ray. The measurements reported in Ref. 2 indicate that the distribution of reflected radiation depends considerably on the angle of incidence.

A calculation which incorporates the actual distribution would be extremely involved and would be restricted to the specific surface. For this reason it is recommended that the data for specular and completely diffuse reflection be used to obtain limiting values for the heat loss. It is also possible to interpolate between these limiting values for a specific surface by assigning a certain fraction of the reflected energy to specular and the rest to diffuse reflection. Distribution curves like the ones presented in Figs. 10 and 11 may be used to make an estimate on these fractions.

ACKNOWLEDGEMENT

The support of the research by the National Science Foundation under grant G10177 is gratefully acknowledged.

REFERENCES

1. E. ECKERT, Messung der Reflexion von Wärmestrahlen an technischen Oberflächen. *Forsch. IngWes.* **7**, 265–270 (1936).
2. BENJAMIN MÜNCH, *Die Richtungsverteilung bei der Reflexion von Wärmestrahlung und ihr Einfluss auf die Wärmeübertragung*, Mitteilungen aus den Institut für Thermodynamik und Verbrennungsmotorenbau an der Eidgenössischen Technischen Hochschule in Zürich, nr. 16 (1955).
3. E. R. G. ECKERT and R. M. DRAKE, JR. *Heat and Mass Transfer*, McGraw-Hill, New York (1959).
4. E. M. SPARROW, J. L. GREGG, J. V. SZEL, and P. MANOS: Analysis, Results and Interpretation for Radiation Between Some Simply Arranged Gray Surfaces, A.S.M.E. paper 60-HT-4. Trans. Amer. Soc. Mech. Engrs., *J. Heat Transfer*, C **83**, May (1961).